HTML ABSTRACT + LINKS

JOURNAL OF APPLIED PHYSICS **97**, 10K311 (2005)

A new approach for improving exchange-spring magnets

J. S. Jiang, J. E. Pearson, Z. Y. Liu, B. Kabius, S. Trasobares, D. J. Miller, and S. D. Bader
Materials Science Division, Argonne National Laboratory, Argonne, Illinois 60439

D. R. Lee, D. Haskel, and G. Srajer
Advanced Photon Source, Argonne National Laboratory, Argonne, Illinois 60439

J. P. Liu
Department of Physics, University of Texas at Arlington, Arlington, Texas 76109

(Presented on 11 November 2004; published online 13 May 2005)

It is demonstrated here that an already ideal exchange–spring magnet can be further improved by intermixing the interface. This is counter-intuitive to the general expectation that optimal exchange–spring magnet behavior requires an ideal, atomically coherent soft–hard interface. Epitaxial Sm–Co/Fe thin-film exchange–spring bilayers are thermally processed, by annealing or high-temperature deposition, to induce interdiffusion. With increasing processing temperature, the hysteresis loop becomes more single-phase-like, yet the magnetization remains fully reversible. The interface is characterized via synchrotron x-ray scattering and electron microscopy elemental mapping. The magnetization behavior is modeled by assuming a graded interface where the material parameters vary continuously. The simulations produce demagnetization curves similar to experimental observations. © *2005 American Institute of Physics*. [DOI: 10.1063/1.1855032]

I. INTRODUCTION

The exchange–spring principle[1] identifies a route for creating high-performance permanent magnets from existing materials rather than by an Edisonian search for new magnetic compounds. In an exchange–spring magnet, nano-scale hard and soft magnetic phases are coupled via interfacial exchange interaction such that the soft phase becomes "hardened" and its high magnetization enhances the energy product $(BH)_{max}$ of the composite. While great efforts have been expended towards controlling the grain sizes during magnet processing, metallurgical approaches such as using nonmagnetic additives come at the expense of forming grain boundary phases and reducing the overall magnetization.[2–4] Concerns about reduced interfacial coupling due to the grain boundary phase also led to the notion that optimal exchange–spring magnets require ideal, atomically coherent soft–hard interfaces.[1,5] However, the soft phase in exchange-springs reverse by nucleating a quasi-Bloch wall, and unlike the Stoner–Wohlfarth case, the exchange field H_{ex} does not depend very sensitively on the interfacial exchange constant.[6] Furthermore, even for an ideal exchange–spring interface, H_{ex} is finite, determined by the soft phase exchange constant and thickness.[7] For an exchange spring with 200 Å of Fe as the soft phase, $H_{ex} \cong 2$ kOe. Thus, there exists a fundamental limit to exchange hardening, and improving the interfacial epitaxy does not overcome the limit.

This limit can, rather counter-intuitively, be circumvented by intermixing the interface. In this article, we demonstrate the enhancement of the nucleation field H_N, and hence $(BH)_{max}$, of epitaxial Sm–Co/Fe bilayers by thermal processing. In contrast to previous studies aimed at interface modification,[8,9] we start with an exchange spring where the interface is already ideal, and create a graded interfacial region where the material parameters vary gradually by promoting intermixing of Sm–Co with Fe. The graded interface has a fundamentally different magnetization behavior than a sharp interface and relaxes the grain size requirement for optimal exchange–spring properties.

II. EXPERIMENTAL DETAILS

The Sm–Co/Fe exchange–spring bilayers were fabricated by dc magnetron sputtering. The nominally Sm_2Co_7 layer was grown epitaxially at 400 °C onto a Cr(211)-buffered single crystal MgO(110) substrate to achieve an in-plane uniaxial anisotropy, as described in Ref. 10. The thickness of the Sm–Co layer in all samples was kept at 20 nm. Following the deposition of the Sm–Co hard layer, a 10 nm- or 20 nm-thick Fe layer was either deposited at 70–100 °C, or immediately at 400 °C. All samples were capped with 10 nm of Ag or Ag(5 nm)/Cr(5 nm) cover layers. Pieces were cut from the as-deposited samples and were annealed for one hour at temperatures ranging from 200 to 400 °C, using the same heater inside the deposition chamber in a vacuum of 1×10^{-8} Torr. We denote a sample by its substrate temperature T_S or annealing temperature T_A, which is the highest temperature the soft layer was subjected to during processing.

The crystal structure and interfacial morphology of the samples were characterized by x-ray diffraction using Cu K_α radiation and by cross-sectional energy-filtered transmission electron microscopy (EFTEM). EFTEM provides the real-space mapping of different elements from the electron energy loss spectra (EELS) at characteristic absorption energies, with a spatial resolution of 0.5 nm. We also extracted the interface width and roughness amplitude parameters by fitting both the specular and off-specular reflectivity measured using synchrotron radiation. The magnetic properties were measured at room temperature by tracing the hysteresis

 © 2005 American Institute of Physics

Downloaded 30 Sep 2005 to 164.54.84.133. Redistribution subject to AIP license or copyright, see http://jap.aip.org/jap/copyright.jsp

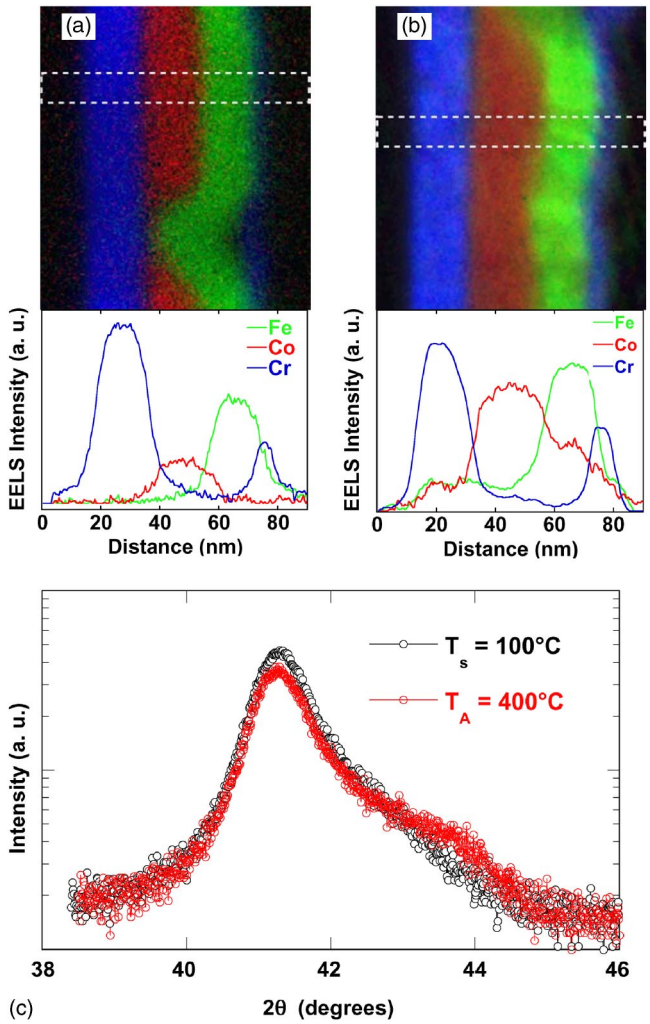

FIG. 1. EELS elemental maps and line scans of Sm–Co(20 nm)/Fe(20 nm) samples with (a) T_S=100 °C and (b) T_A=400 °C. The line scans are taken from the 9 nm×90 nm area enclosed by the dashes. (c) Comparison of the high-angle x-ray diffraction of the two samples measured around the Sm–Co(2$\bar{2}$00) peak.

loops and the dc demagnetization remanence (DCD) curves using an alternating gradient magnetometer with the field applied along the easy direction of the Sm–Co layer. For the DCD curves, the samples were saturated with a +1.4 T field each time before a demagnetizing field was applied, then the remanent magnetization was measured and plotted as a function of the demagnetizing field.

III. RESULTS AND DISCUSSION

The epitaxial Sm–Co/Fe bilayers are a model exchange–spring system with ideal, coherent interfaces.[11,12] The Sm–Co layer grows initially in an islanding mode with large roughness.[10] When the Fe layer is deposited at a low T_S, the Sm–Co/Fe interface is expected to be sharp but jagged. Annealing or depositing the Fe layer at elevated temperatures promotes interdiffusion between the Sm–Co and Fe, blurring the interface and reducing the roughness. These microstructural characteristics are immediately evident in the cross-sectional EFTEM images shown in Fig. 1 for two Sm–Co(20 nm)/Fe(20 nm) samples with T_S=100 °C, and

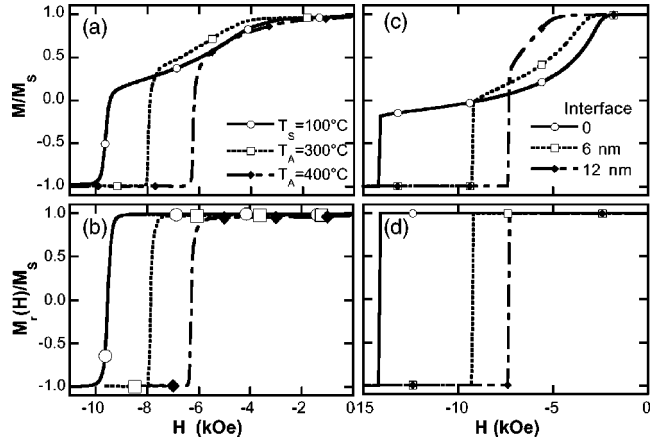

FIG. 2. (a) The demagnetization and (b) the dc demagnetization remanence curves for Sm–Co(20 nm)/Fe(10 nm) samples annealed at various temperatures. (c) The demagnetization and (d) the dc demagnetization remanence curves calculated for Sm–Co(20 nm)/Fe(10 nm) bilayers with interfacial regions of various thickness.

T_A=400 °C. The images are constructed from the EELS spectra and color-coded to represent the spatial distribution of the elements Fe, Co, and Cr. The Co map (red) shows the notch in the T_S=100 °C sample due to interfacial roughness, whereas the T_A=400 °C sample has a diffuse boundary between the Fe (green) and Co maps and a notch is blurred out. The difference in interdiffusion in the samples can be seen more clearly in the 9 nm-wide line scans. In the T_S=100 °C sample the layers are well-defined, but in the T_A=400 °C sample Fe is found in the entire Sm–Co layer while the amount of Co entering into the Fe layer decreases with distance from the interface. Synchrotron reflectivity measurements show similar total interface width of ~2.5 nm for both samples, but roughness amplitude of 2.0 nm for the T_S=100 °C sample and 0.7 nm for the T_A=400 °C sample. High angle x-ray diffraction of the T_A=400 °C sample shows a broad shoulder to the right of the Sm–Co(2$\bar{2}$00) peak. The shoulder could not be fitted with a single Gaussian curve, suggesting a distribution of phases with smaller lattice constants. While the EELS elemental maps provide the structural characteristics over the limited field-of-view of EFTEM, the scattering techniques average over the macroscopic area on the samples illuminated by the x-ray. The consistency among the results from the three techniques proves conclusively that the Sm–Co/Fe interface evolves from being sharp but jagged to smoother and interdiffused upon thermal processing at elevated temperatures.

Shown in Fig. 2(a) are the demagnetization branches of the hysteresis loops for Sm–Co(20 nm)/Fe(10 nm) samples with T_S=100 °C, T_A=300 °C, and 400 °C. At T_A=300 °C, the onset of the Fe layer reversal increases to over 4 kOe from under 3 kOe for the T_S=100 °C sample, while the switching field of the hard layer becomes reduced. After annealing at 400 °C, the hysteresis becomes single-phase like with the coercivity greater than 6 kOe. The measured room-temperature saturation magnetization (M_s) for all samples of this composition is ~930 emu/cm^3. The $(BH)_{max}$ value increases from 24 MGOe for the T_S=100 °C sample to 27.7 MGOe for the T_A=300 °C sample, and then decreases

Downloaded 30 Sep 2005 to 164.54.84.133. Redistribution subject to AIP license or copyright, see http://jap.aip.org/jap/copyright.jsp

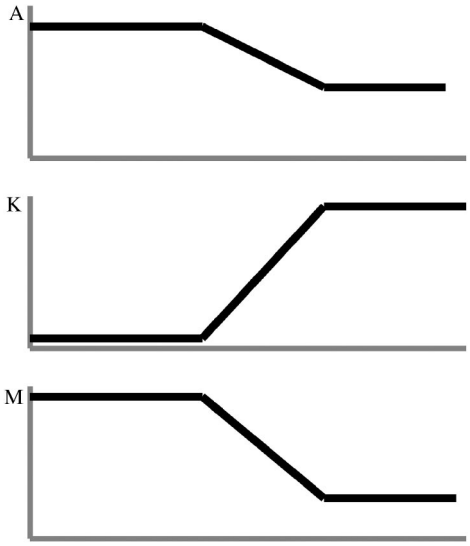

FIG. 3. Schematic illustration of the variation in exchange (A), anisotropy (K) and magnetization (M) across a graded Sm–Co/Fe interface.

to 22.4 MGOe for the 400 °C sample. Note that although the mathematical limit of $(BH)_{\max}$ for Sm–Co/Fe of this composition is 34 MGOe, $(BH)_{\max}$ is only 21 MGOe for an ideal exchange spring.[11] Annealing has made up nearly 50% of the difference. The DC demagnetization remanence curves, which measure the reversibility of the magnetization, are shown in Fig. 2(b). All samples have sharp step-like DC demagnetization remanence curves, indicating a very narrow distribution of the hard layer switching fields and full reversibility of the soft layer magnetization. Particularly noteworthy is the sample with $T_A = 400$ °C. It has a nearly square demagnetization loop, yet the magnetization is fully reversible. In contrast, most nanophase hard magnets show significant irreversible magnetization due to partial reversal of the hard phase, even though their hysteresis loops may appear single-phase-like.[2,9] A similar trend with thermal processing is observed in exchange–springs with thicker Fe layers. For Sm–Co(20 nm)–Fe(20 nm) samples with $T_S = 70$ °C, $T_A = 300$ °C, and $T_S = 400$ °C, the H_N and $(BH)_{\max}$ values are 1 kOe and 9.4 MGOe, 1.2 kOe and 12 MGOe, 1.6 kOe and 14.1 MGOe, respectively.

We simulated the demagnetization behavior of these bilayers using the one-dimensional spin-chain model described in Ref. 11. Based on structural and compositional characterization, we model the interdiffused interface with a graded profile for the intrinsic material parameters, where the exchange constant A, the magnetic anisotropy K, and the magnetization M ramp linearly, from those of the Fe to those of the Sm–Co, as depicted in Fig. 3. The end values for A, K, and M are the same as those used for Fe and Sm–Co in Ref. 11, and the width of the interfacial region reflects the extent of interdiffusion. The results for three Sm–Co(20 nm)/Fe(10 nm) bilayers with different interface width are plotted in Figs. 2(c) and 2(d). The simulated demagnetization and DCD curves closely resemble those measured experimentally. The measured demagnetization curve becomes more single-phase-like with increased processing temperature, and the same trend is seen in the simulated loops for increased interface width. The results of intermixing are that the anisotropy increases and magnetization decreases in the part of the interfacial region which used to be soft Fe, leading to an increase of H_N, and therefore, $(BH)_{\max}$.

The exchange–spring principle exemplifies the "materials-by-design" approach in materials research. The extent of exchange hardening in exchange–spring magnets is ultimately limited by the physics of magnetization reversal. The graded-interface scheme presented here calls for the nano-scale control of material parameters to change the magnetization behavior and to circumvent the limit. The remedial nature of interfacial modification means that it can be carried out post-processing, thereby overcoming the difficulty in grain size control encountered by conventional magnet processing routes.

IV. CONCLUSION

We show that an ideal, atomically coherent soft–hard interface is not the prerequisite for optimal exchange–spring behavior. By creating an interdiffused interface in initially epitaxial Sm–Co/Fe bilayers via thermal processing, we increase the nucleation field, hence improving the energy product above that expected of an ideal exchange-spring. We have modeled the effect of thermal processing with a graded interfacial region and have qualitatively reproduced the experimental observations.

ACKNOWLEDGMENTS

The work at Argonne was supported by the U.S. DOE BES-MS under Contract No. W-31-109-ENG-38. We thank Y. Choi for assistance with the reflectivity measurements. EFTEM was carried out at the Electron Microscopy Center at Argonne National Laboratory. J. P. L. acknowledges support by the U.S. DOD/DARPA under Grant No. DAAD 19-01-1-0546.

[1] E. F. Kneller, R. Hawig, IEEE Trans. Magn. **27**, 3588 (1991).
[2] For a review, see G. C. Hadjipanayis, J. Magn. Magn. Mater. **200**, 373 (1999).
[3] A. Zern, M. Seeger, J. Bauer, and H. Kronmüller, J. Magn. Magn. Mater. **184**, 89 (1998).
[4] O. Gutfleisch, J. Phys. D **33**, R157 (2000).
[5] R. Fischer and H. Kronmüller, J. Appl. Phys. **83**, 3271 (1998).
[6] T. Nagahama, K. Mibu, and T. Shinjo, J. Phys. D **31**, 43 (1998).
[7] E. Goto, N. Hayashi, T. Miyashita, and K. Nakagawa, J. Appl. Phys. **36**, 2951 (1965).
[8] J. Kim, K. Barmark, M. De Graef, L. H. Lewis, and D. C. Crew, J. Appl. Phys. **87**, 6140 (2000).
[9] D. C. Crew, J. Kim, L. H. Lewis, and K. Barmak, J. Magn. Magn. Mater. **233**, 257 (2001).
[10] E. E. Fullerton, J. S. Jiang, C. Rehm, C. H. Sowers, S. D. Bader, J. B. Patel, and X. Z. Wu, Appl. Phys. Lett. **71**, 1579 (1997).
[11] E. E. Fullerton, J. S. Jiang, and S. D. Bader, J. Magn. Magn. Mater. **200**, 392 (1999).
[12] M. J. Pechan, N. Teng, J.-D. Stewart, J. Zachary Hilt, E. E. Fullerton, J. S. Jiang, C. H. Sowers, and S. D. Bader, J. Appl. Phys. **87**, 6686 (2000).

Downloaded 30 Sep 2005 to 164.54.84.133. Redistribution subject to AIP license or copyright, see http://jap.aip.org/jap/copyright.jsp